Characterization of silicon micro-ring resonators

Westerveld, W. J.; Pozo, J.; Leinders, S. M.; Yousefi, M.; Urbach, H. P.

Publication date
2013

Document Version
Final published version

Published in
Proceedings of the 18th Annual Symposium of the IEEE Photonics Society Benelux

Characterization of silicon micro-ring resonators

W.J. Westerveld[1,2] J. Pozo[2] S.M. Leinders[1] M. Yousefi[3] and H.P. Urbach[1]

[1] Delft University of Technology, Van der Waalsweg 8, 2628CH Delft, The Netherlands
[2] TNO, Stieltjesweg 1, 2628CK Delft, The Netherlands
[3] Photonic Sensing Solutions, Haarlemmerstraat 141, 1013EN Amsterdam, The Netherlands

Silicon micro-ring resonators are now widely used and studied as filters in the field of optical communication and as sensitive elements in the field of sensing. This work aims to provide silicon photonic designers with a set of results and reasoning to assist them with the design of micro-rings. We fully and detailedly characterized waveguide, waveguide bends, and directional couplers including their dispersion. The chip was fabricated via the ePIXfab platform. To the best of our knowledge, we are the first to report on the exceptional phase shift of directional couplers in the situation when they are used as cross-coupler.

Introduction, devices, and setup

Silicon photonic micro-ring resonators receive large interest [1]. In this work, we present a methodology to characterize the components of such resonators and the obtained set of figures.

We characterized integrated optical devices in silicon-on-insulator technology, having 220 nm thick rectangular waveguides. The devices were fabricated via the EU-funded ePIXfab consortium at IMEC (Leuven) in their IMEC8 multi-project-wafer shuttle. IMEC fabricated the devices in their semi-industrial CMOS line with deep-UV lithography. We measured the dimensions of the waveguides with a helium-ion-microscope (Carl Zeiss SMT), providing 15 nm accuracy. We deposited a 2 μm thick SiO_2 cladding using plasma-enhanced chemical vapor deposition (PECVD). However, the disagreement between the measured coupling of directional couplers and the simulated coupling suggests that the PECVD may be imperfect. The main concern is the deposition of SiO_2 in the small gap between the waveguides.

The photonic chips have out-of-plane grating couplers [2] and are measured in an automated setup to the provide high alignment repeatability that is necessary for loss measurements [3]. The fibers are manually positioned above the chip for a set of consecutive measurements. Fine in-plane alignment is achieved by sequentially scanning the 4 in-plane axis of the two piezo-actuated stages to maximize the transmitted power. We used amplified spontaneous emission (ASE) light-source and recorded the transmittance spectra around $\lambda_c = 1550$ nm free-space wavelength with an optical spectrum analyzer (OSA).

Loss characterization

The devices in Fig. 1a only differ in the length l' of the straight waveguides, with a total length difference of 5 cm. Transmission spectra of these devices were recorded and averaged over 5 nm wavelength spans to remove the "noise" originating from spurious reflections. The loss per length was found by linear fitting of the transmitted power versus

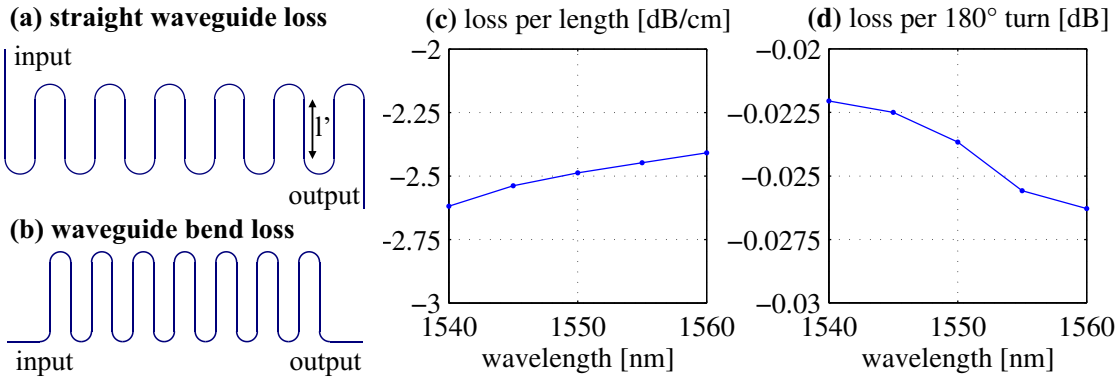

Figure 1: Sketch of devices for measuring loss of straight **(a)** and bend **(b)** waveguides with 397 nm. Measured loss in straight **(c)** and bend **(d)** waveguides (radius 5 μm).

the length of the straight waveguides. The average loss over the 25 nm wavelength span is -2.50 dB/cm and there is only a weak wavelength dependence (Fig. 1c). This loss is slightly higher than the values reported in literature [4], possibly because our waveguides are 60 nm smaller and our SiO_2 cladding deposition is not optimized. Loss in waveguide bends are characterized by comparing the transmission through waveguides with a different number of bends (Fig. 1b, with upto 359 bends). The transmission is compensated for the loss in the straight waveguides and the loss per 180° turn is found by linear fitting. The averaged loss is -0.024 dB/turn with low wavelength dependency (Fig. 1c).

Directional coupler characterization

A directional coupler consists of two parallel waveguides so close that power couples from one waveguide to the other via the evanescent fields of the modes (Fig. 2a). Using coupled mode theory, the total electric field is approximated by a superposition of the two modes of the isolated waveguides. Lossless couplers have straigh-through power $|t|^2$, coupled power $(1-|t|^2)$, and a straight-trough amplitude transmission t given by [5]

$$t = e^{-\imath(\beta_b+\kappa_{bb}-\delta)\tilde{L}}\left(\cos s\tilde{L} - \imath\delta/s\cdot\sin s\tilde{L}\right), \tag{1}$$

with β_b the propagation constant of the lower waveguide, κ_{bb} a correction on β_b due to the vicinity of the other waveguide, 2δ the difference between the corrected propagation constants of the two waveguides, s the coupling coefficient, $\tilde{L} = L + \Delta L$ the effective length of the coupler, where L is the length of the parallel waveguides, and ΔL is a correction for the coupling occurring in the bends. The correction κ_{bb} is smaller than the fabrication-induced uncertainty in β_b, hence we neglect $\kappa_{bb} \ll \beta_b$. Dispersion in waveguide propagation constant β_b is taken into account by assuming linear dispersion of the effective index $n_e(\lambda)$, hence $\beta_b(\lambda, n_e, n_g) = 2\pi\left((n_e - n_g)/\lambda_c + n_g/\lambda\right)$, with n_e and $n_g \equiv n_e - \lambda(\partial n_e/\partial\lambda)$ evaluated at λ_c. Dispersion in the coupling $s(\lambda) = s + s'(\lambda - \lambda_c)$ is assumed linear. We neglect dispersion in ΔL, which is validated by the fact that the obtained relations accurately describe the measured spectra. We measured directional couplers in ring resonators (Fig. 2b) having power transmission T given by [5]

$$T = \left(\alpha^2 + 1 - 2\alpha\cos\theta\right)|t|^2 / \left(1 + \alpha^2|t|^4 - 2\alpha|t|^2\cos\theta\right)\cdot P_0, \tag{2}$$

with α the round-trip amplitude transmission of the ring ($\alpha = 1$ means no loss), $|t|$ the amplitude transmission through the coupler, θ the round-trip phase delay of the ring in-

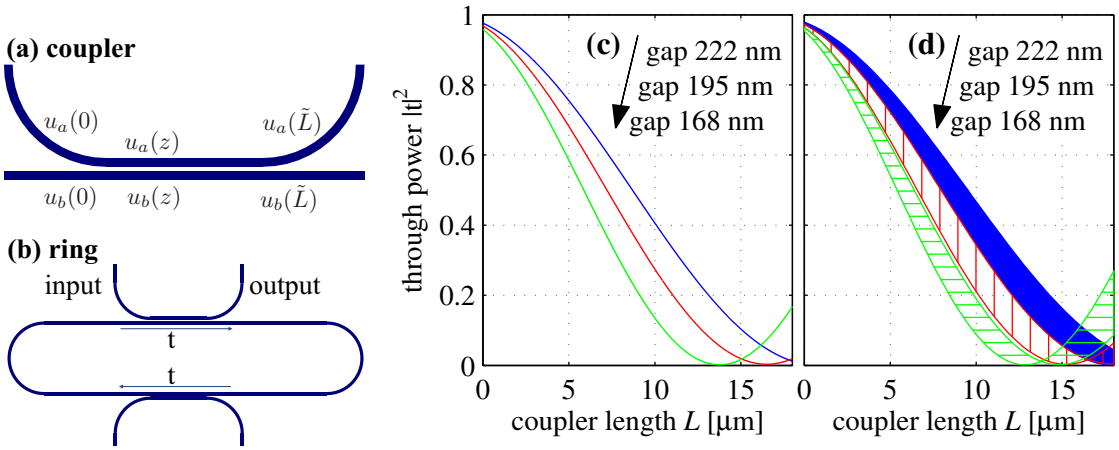

(e) Fitted parameters

gap [nm]	width [nm]	s [μm^{-1}]	ΔL [μm]	s' [μm^{-2}]	δ [μm]	n_g
222	391	0.073	2.134	0.339	0.0006	4.319
195	392	0.084	2.118	0.411	0.0048	4.319
168	394	0.099	2.053	0.414	0.0042	4.313

Figure 2: Directional coupler characterization. **(a)** Sketch of coupler. Waveguide width ∼400 nm and bending radius 5 μm. **(b)** Sketch of ring with two couplers. 40 μm straight waveguides and 5 μm bending radius. **(c)** and **(d)** Straight-through transmission power $|t|^2$ of the directional coupler for $\lambda_c = 1550$ nm and $\lambda_c \pm 15$ nm, respectively. **(e)** Table of fitted parameters.

cluding the two couplers, and P_0 the power in the input waveguide. For a ring with two directional couplers, the phase delay θ is, using Eq. (1),

$$\theta = -\beta_b l + 2\delta\tilde{L} + 2\arg\left\{\cos s\tilde{L} - \imath\delta/s \cdot \sin s\tilde{L}\right\}. \tag{3}$$

We measured three sets of couplers with different gaps and similar waveguides. Each set consists of eleven devices with coupler length L varying from 0 μm to 18 μm. Equation (2 with 3 and 1) was fitted fitted to the set of spectra. Transmittance α was calculated using Fig. 1, leaving unknowns s, ΔL, s', δ, n_g, $\{n_e\}$ and $\{P_0\}$. The effective index n_e and input power P_0 vary from device to device due to variations in fabrication [1] and in fiber-chip alignment, respectively, while the other unknowns share single values for all spectra. Levenberg-Marquardt optimization is used to minimize the squared difference between the measured and computed spectra $T(\lambda)$. To weight all spectra approximately equally, we weighted each datapoint (wavelength) with $1/I$, with I the average intensity in a 5 nm span around this wavelength. An accurate initial guess is necessary, which we obtained using less complete analysis neglecting dispersion and asymmetry in the coupler ($\delta = 0$, $s' = 0$), and by choosing $\{n_e\}$ and n_g to match the wavelengths of the resonance dips in the recorded spectra.

Fig. 3 shows that the fitted spectra agree very well with the measured spectra, indicating that the theory indeed contains all important effects. Length $L = 8$ μm shows a typical spectrum with a FSR of 5.0 nm, but $L = 14$ μm is in the particular cross-coupling regime with nearly all light coupled to/from the ring ($|t|^2 \approx 0$). The change in FSR is due to the additional phase delay of the directional couplers (Fig. 3c). We define the third term on the right-hand-side of Eq. (3) as this additional phase delay, which only occurs for couplers with asymmetry between its waveguides ($\delta \neq 0$). We designed the two waveguides

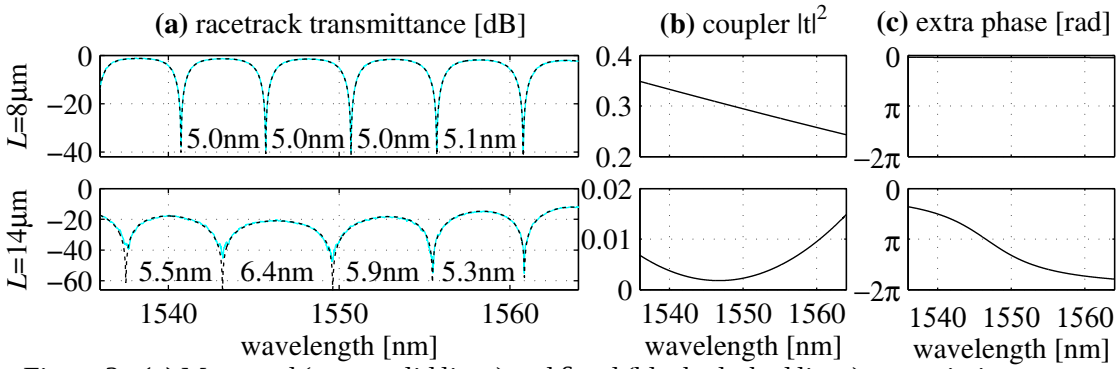

Figure 3: **(a)** Measured (cyan, solid lines) and fitted (black, dashed lines) transmission spectra of the ring resonators (two different coupler lengths L). Normalized to the transmission of a single-mode waveguide. **(b)** and **(c)** Quantities obtained from the fitted curve.

to be identical ($\delta = 0$) but observed small a asymmetry δ. This additional phase delay is usually negligible as the real part inside this argument is much smaller than the imaginary part ($\delta \ll s$), but around $|t| \approx 0$, we have $\cos s\tilde{L} = 0$ so that the real part vanishes and the phase delay rapidly increases. In one spectrum, $\tilde{L}$ is fixed but s varies slightly due to linear dispersion s'. The straight-through power of the coupler $|t|^2$ is plotted in Fig. 3b, and the wavelength of minimal transmission agrees with the rapid variation in additional phase delay (Fig. 3c) and with the corresponding change in the FSR (Fig. 3a). This significant change is explained by a small difference between the corrected propagation constants of the waveguides, $2\delta/\beta$, of 0.1%. To get a feeling for δ, we numerically compute the difference in the widths of the waveguides Δw that would give such an asymmetry, giving $\Delta w \approx \partial w/\partial\beta \cdot 2\delta = 1$ nm.

Fig. 2e shows the fitted unknowns and Fig. 2c shows the corresponding behavior of the couplers. Fig. 2d presents their wavelength dependency, showing a variation in the coupled power ($1 - |t|^2$) up to 0.18 within the wavelength span of 30 nm.

Conclusion

We measured propagation loss of straight and bent waveguides and observed a weak wavelength dependency. We characterized directional couplers using an analysis based on coupled-mode-theory and found excellent agreement between the measured spectra and the theoretical shape, indicating that all relevant physics is included. The couplers showed significant wavelength dependency. We demonstrated that a tiny (nanoscale) asymmetry in the two waveguides of a coupler causes a significant additional phase delay in the cross-coupling regime where most light is coupled from one waveguide to the other.

We acknowledge the ePIXfab consortium for the fabrication of the devices, with special thanks to dr. Pieter Dumon and dr. Amit Khanna of IMEC (Leuven). At TNO (Delft), we thank ing. Hans van den Berg, dr. Emile van Veldhoven, dr. Peter Harmsma, and ir. Remco Nieuwland.

[1] W. Bogaerts *et al.*, "Silicon microring resonators," *Laser & Photonics Reviews*, vol. 6, p. 47, 2012.
[2] D. Taillaert, P. Bienstman, and R. Baets, "Compact efficient broadband grating coupler for silicon-on-insulator waveguides," *Optics Letters*, vol. 29, p. 2749, 2004.
[3] W. J. Westerveld, "Silicon integrated optomechanical sensors," Presented at the European Conference on Optical Communication (ECOC), workshop WS07, Amsterdam, Sep. 2012, (*invited*).
[4] W. Bogaerts and S. Selvaraja, "Compact single-mode silicon hybrid rib/strip waveguide with adiabatic bends," *Photonics Journal, IEEE*, vol. 3, p. 422, 2011.
[5] A. Yariv and P. Yeh, *Photonics*. Oxford University Press, 2007.